



Optimal GLCM combined FCM segmentation algorithm for detection of kidney cysts and tumor

Paladugu Raju¹ · Veera Malleswara Rao² · Bhima Prabhakara Rao³

Received: 14 December 2017 / Revised: 24 October 2018 / Accepted: 28 December 2018 /

Published online: 28 January 2019

© Springer Science+Business Media, LLC, part of Springer Nature 2019

Abstract

In this document, we employed an efficient Optimal GLCM attribute related FCM segmentation algorithm which is used to categorize the kidney cysts and tumor from the ultrasound kidney images. The FCM is exploiting some appropriate attributes of GLCM texture feature extractor and optimally attach the cluster centroids of FCM by the help of Whale optimization algorithm. The proposed approach is executed in the working platform of Matlab. The findings demonstrate that the proposed model have better performance in recognizing the detection of kidney cysts and tumor in patients by examining US kidney images. Also, we have shown the comparison of our proposed method FB-FCM-WOA with the existing methodologies like FB-FCM, FB-K-means, IB-FCM and IB-K-means. Hence, we would suggest that our proposed method is much better for detecting kidney cysts and tumor.

Keywords Feature based Fuzzy C-means (FbFCM) · Whale Optimization algorithm (WOA) · Gray Level Co-occurrence Matrix (GLCM) · Ultrasound (US) kidney tumor and cyst segmentation

1 Introduction

Nowadays, the world is suffering dissimilar kind of kidney diseases. Generally, the kidney is the majority dangerous organ in urinary system, which contributes the complete body homeostasis, maintaining corrosive base balance, electrolyte focuses, extracellular fluid volume, and blood pressure. Here, the kidney encompasses four distinctive segments among diverse capabilities such as renal cortex, renal column, renal medulla, and renal pelvis [10]. After the occurrence of kidney

✉ Paladugu Raju
praju0817@gmail.com

¹ Department of ECE, JNTUK Kakinada, Kakinada, Andhra Pradesh 533003, India

² Department of ECE, GIT, GITAM Deemed to be University, Visakhapatnam, Andhra Pradesh 530045, India

³ Programme Director, Nanotechnology, JNTUK Kakinada, Kakinada, Andhra Pradesh 533003, India

diseases, the kidneys are injured and can't filter blood properly. So, it augments the waste in the body [14]. Normally, most of the people don't observe indication in its earlier phase. Therefore, it instigates to damage kidney steadily. But, these kinds of kidney disease are mostly requiring premature detection and remedial accomplishment [21]. The premature detection of kidney disease is allowing a more possible and suitable handling to the patient [19].

At the present time, the advance robotized systems like ultrasonic systems are used to detect the kidney diseases which authorize a major computation and data removal in the patients. The exploitation of attribute removal, image inspection, and model identification policy for grouping are considered as the appropriate evaluation of universal circumstances (e.g. disappointment, stone, tumor, and cyst) [2]. Feature extraction is a fundamental progression for US kidney image processing. Feature extraction is used to divide the noticeable attributes from the dissimilar collection of attributes by their pixel intensity association [11]. Therefore, several works are completed through professionals in the US image extraction. In kidney US images, the removed attributes are encompassing unique attributes, geometric minute attributes, and area gray appropriation. Normally, the typical set of kidney US image is exploited for feature extraction which is rely on five intensity histogram attributes and nineteen gray level co-occurrence matrix (GLCM) attributes [11].

In the medical field, several identification policies are available at current. Every process is based upon the significance of kidney disease at precise time [21]. A major purpose of image processing is to improve the appearance of an image, thus, there is a lot of image processing tools. Image Processing Tools aids engineers and scientists with an extensive set of plugin, toolkit, functions, and apps for image processing, analysis. Some of the image segmentation tools are VTK, ITK, FSL, SPM, GIMIAS, Elastix etc. [16].

Kidney segmentation is considered as a difficult task in Magnetic Resonance (MR) datasets because the consequence of incomplete volume problem, intensity in-homogeneity, and spillage of discrimination mediator to adjacent organs, high signal to clamor rate, additional curios, and a small gradient response [7]. Segmentation of kidney ultrasound picture is mainly taking place by dissimilar policy in texture assessment, dynamic shape procedure, area development policy, level set policy, and spline structure policy. Region growing is the position which is accumulating pixels as larger section. Furthermore, it exploits the spatial data and makes sure the collection of shut related sections [20, 26].

Clinical assessment of ultrasound kidney images with comparable intensities is also considered as a disadvantage in the segmentation progression, which is specified the low dissimilarity among kidney and its adjacent arrangement. Therefore, it is significant to discover a suitable segmentation process for to develop the segmentation exactness and kidney assessment. In this document, we have employs an effectual Optimal GLCM feature related FCM segmentation algorithm for the classification of kidney cysts and tumor from the ultrasound kidney images. The rest of this paper is organized as follows: In Section 2, we briefly describe about the existing approaches and related works. The proposed method is described in Section 3. In Section 4, we present our experimental results. Some concluding remarks are presented in Section 5.

2 Related work

Here, we have discussed some of the related works in the detection of kidney cysts and tumor collected from medical images which were depicted below,

Torres, Helena R., et al. [24] has proposed a methodical investigation of various procedures for kidney segmentation. In medical images, diverse processes are used to divide the kidney from exacting imaging acquisition systems like ultrasound, magnetic, resource, and registered tomography. It was proposed to analyze and regulate by various kidney segmentation algorithms, arrange an assessment with them and converse regarding the appropriate procedures for each modality. It was feasible to discriminate the segmentation methods by exacting image processing module which is exploited to divide the kidney in images of diverse imaging modalities.

Marsousi Mahdi et.al [18] has introduced a systematic and cost-effective method capable of detecting and segmenting the kidney's shape in acquired 3-D ultrasound volumes, using off-line training datasets. They offered a new shape model representation, called the complex-valued implicit shape model, to generate a 3-D kidney shape model by combining prior knowledge of training shapes and anatomical knowledge. They applied shape-to-volume registration, based on a new similarity metric, to detect the kidney shape by fitting the 3-D shape model on 3-D ultrasound volumes. Upon kidney detection, the fitted shape model was used to initialize and evolve a new level-set function, called complex-valued rational level-set with shape prior, to segment the kidney's shape.

Jin Chao et.al [3] has exhibited a fully automatic method to segment the kidney into multiple components: renal cortex, renal column, renal medulla and renal pelvis, in clinical 3D CT abdominal images. The developed fast automatic segmentation method of kidney consists of two main parts: localization of renal cortex and segmentation of kidney components. In the localization of renal cortex phase, a method which fully combines 3D Generalized Hough Transform (GHT) and 3D Active Appearance Models (AAM) was applied to localize the renal cortex. In the segmentation of kidney components phase, a modified Random Forests (RF) method was presented to segment the kidney into four components based on the result from localization phase.

Lin Daw-Tung et.al [17] has developed an effective model-based approach for computer-aided kidney segmentation of abdominal CT images with anatomic structure consideration. This automatic segmentation system was expected to assist physicians in both clinical diagnosis and educational training. This method was a course to fine segmentation approach divided into two stages. First, the candidate kidney region was extracted according to the statistical geometric location of kidney within the abdomen. This approach was applicable to images of different sizes by using the relative distance of the kidney region to the spine. The second stage identifies the kidney by a series of image processing operations. The main elements of the presented system are: 1) the location of the spine was used as the landmark for coordinate references; 2) elliptic candidate kidney region extraction with progressive positioning on the consecutive CT images; 3) novel directional model for a more reliable kidney region seed point identification; and 4) adaptive region growing controlled by the properties of image homogeneity.

Khalifa, Fahmi, et al. [13] have proposed a regional attribute from the CT form, a kidney shape prior representation, and higher-order spatial communications which were removed and exploited for tissue classification. Here, the shape show was enhanced by means of a collection of preparation images which was revitalized in the middle of segmentation through an exterior-related policy of both voxels' position and form. The spatial communications among CT information voxels are exhibited by means of a higher-order spatial representation which includes the pair wise set of the triple-and quad set.

Krishna K. Divya et.al [5] has developed an FPGA based CAD algorithm for abnormality detection of kidney in ultrasound images. The presented algorithm works in the following way: as a pre-processing, an ultrasound image is denoised and region of interest of kidney in ultrasound image was segmented. Intensity histogram features and Haralick features were extracted from the segmented kidney region. Based on extracted features, the classification algorithm was implemented in two stages. In first stage, a Look Up Table (LUT) based approach was used to differentiate between normal and abnormal kidney images. In second stage, after confirming the abnormality, Support Vector Machine (SVM) with Multi-Layer Perceptron (MLP) classifier trained with extracted features was used to further classify the presence of stone or cyst in kidney.

Song Hong et.al [9] have presented a coarse-to-fine method was applied to segment kidney from CT images, which consists two stages including rough segmentation and refined segmentation. The rough segmentation was based on a kernel fuzzy C-means algorithm with spatial information (SKFCM) algorithm and the refined segmentation was implemented with improved Grow Cut (IGC) algorithm. The SKFCM algorithm introduces a kernel function and spatial constraint into fuzzy c-means clustering (FCM) algorithm. The IGC algorithm makes good use of the continuity of CT sequences in space which can automatically generate the seed labels and improve the efficiency of segmentation.

3 Proposed FbFCM-WOA method for cyst/tumor segmentation in US kidney images

The block diagram of Proposed segmentation process using Optimal GLCM attribute related FCM segmentation algorithm is specified in the underneath Fig. 1.

In segmentation, the images are transformed as 3×3 blocks and the attributes are removed. The FbFCM employs some significant attributes of GLCM texture features and optimally unites the group centroids of FCM using Whale optimization algorithm to improve segmentation accuracy. The GLCM texture attributes are removed for the entire image blocks. Here, the preliminary centroid of FbFCM is considered as the attribute vector of image sub-blocks. The intensity of ultrasound kidney image is discriminating the background segment, tumor/cyst segment, and the adjacent kidney segment. So, it is divided as three dissimilar sections. Here, we can simply observe the tumor/cyst segment from the three-image clustered segment of kidney images through setting up the quantity of clusters as 3.

Therefore, the three main steps of the proposed FbFCM segmentation method are of,

- Image Block conversion
- GLCM Feature extraction
- FbFCM-WOA based segmentation

Each stage of proposed FbFCM segmentation method is detailed in the upcoming sections.

3.1 Image block conversion

In this preliminary step, the proposed block related segmentation process is the block conversion. Here, the input ultrasound kidney images (i.e. kidney tumor/cyst images) are divided as a quantity of sub- images with identical sizes. At this point, the image of size $256 \times$

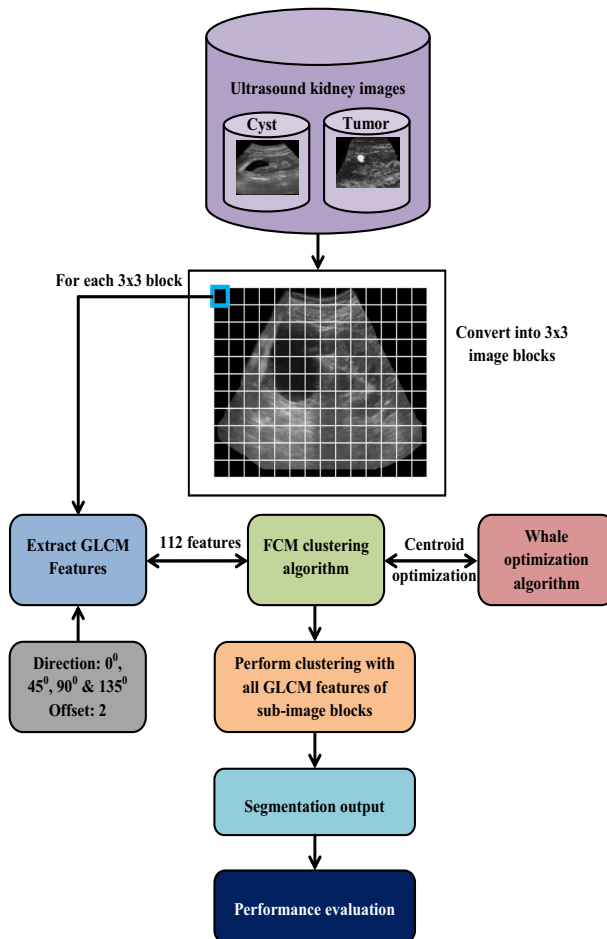


Fig. 1 Schematic diagram

256 is transformed as 3×3 blocks and every block is performed as independently. In attribute removal, the GLCM attributes are removed for every sub-block.

3.2 GLCM feature extraction

Grey Level Co-occurrence Matrices (GLCM) are one of the earliest techniques used for image texture analysis in which texture is an important characteristic used in identifying regions of interest in an image. In this paper, the Gray-Level Co-occurrence Matrix (GLCM) is a distinguished arithmetical procedure for attribute removal. The GLCM is considered as dissimilar amalgamation of pixel gray levels in an image. The foremost objective of the method is to allocate an unidentified model image to a group of texture features which is distinct by its distinctive possessions. Additionally, they distinguish the textural possessions of images as spatial arrangement, contrast, roughness, orientation, etc. which are containing convinced association through the preferred output [15]. At this point, the GLCM attributes are removed for segmentation process which is derived from the attributes of sub-blocks. The

comparable image segments are classified as three groups. Moreover, the kidney images are divided as three disparate segments. Therefore, the three disparate segments are considered as three diverse image segments such as, (i) background segment; (ii) tumor/cyst segment and; (iii) kidney segment.

GLCM is distinct as the component position, (i, j) in GLCM which specified the frequency of two pixels in an exact window. Here, one pixel grayscale value is ' i ', and the further pixel grayscale value is ' j ' and the adjacent detachment of ' o ' in the ' ψ ' direction. Normally, ' o ' obtains 1 or 2, and ψ acquire the four directions value of 0° , 45° , 90° and 135° . Here, the offset ' o ' is choose as 2 and the entire four directions are used to remove the image attributes. Therefore, two groups of GLCM matrix values are initiated.

All element values of GLCM are determined as follows:

$$R(i, j) = \frac{G(i, j, o, \psi)}{\sum_{i=1}^H \sum_{j=1}^H G(i, j, o, \psi)} \quad (1)$$

From formula (1), $G(i, j, o, \psi)$ is the frequency of double component position where the pixel grayscale value is ' i ' and ' j ' and the adjacent detachment to ' o ' in the ' ψ ' direction; and H is the quantity of gray levels in the image. Moreover, $R(i, j)$ is the $(i, j)^{th}$ component of GLCM matrix.

In the GLCM matrix, 14 possible attributes are obtained at four dissimilar orientations and two offsets. The 14 attributes are Inverse Difference Moment, Contrast, Entropy, Energy, Sum Average, Sum Entropy, Sum of squares, homogeneity, correlation, autocorrelation, cluster shade, maximum probability, difference variance, difference entropy [6]. Therefore, the 112 features (i.e. $2(\text{offset}) * 4(\text{direction}) * 14$) are obtained for every sub-image blocks. A few GLCM attributes are specified in the subsequent segment [27].

3.2.1 Entropy

Entropy is the quantity of image information which is required for the image compression. Entropy is used to calculate the failure of information or message in a transmitted signal and the image information.

$$Entropy = -\sum_{i=0}^{H-1} \sum_{j=0}^{H-1} R(i, j) * \log(R(i, j)) \quad (2)$$

3.2.2 Angular second moment

Angular Second Moment is the sum of squares of entries in the GLCM which is used to compute the image homogeneity. It is also recognized as Uniformity or Energy. Suppose, if an image encompasses very good homogeneity or pixels are very comparable, then Angular Second Moment is high.

$$ASM = \sum_{i=0}^{H-1} \sum_{j=0}^{H-1} R(i, j)^2 \quad (3)$$

3.2.3 Contrast

Contrast is used to compute the quantity of local alteration in an image which imitates the sensitivity of textures with the intensity. It precedes the evaluation of intensity contrast among a pixel and its region.

$$Contrast = \sum_{n=0}^{H-1} n^2 \left\{ \sum_{i=1}^H \sum_{j=1}^H R(i, j) \right\}, |i-j| = n \quad (4)$$

Here, $R(i, j)$ is the Co-occurrence Matrix, which is used to compute the contrast or local intensity dissimilarity from $R(i, j)$ of diagonal, i.e. $i \neq j$.

3.2.4 Correlation

Correlation is the linear dependency in grey levels of adjacent pixels. The correlation can be specified by the subsequent equation,

$$Correlation = \sum_{i=0}^{H-1} \sum_{j=0}^{H-1} \frac{[i*j] * (R(i, j)) - [\mu_x * \mu_y]}{\sigma_x * \sigma_y} \quad (5)$$

Where, μ_x, μ_y and σ_x^2, σ_y^2 are the mean and variance of i, j , are given as,

$$\begin{aligned} \mu_x &= \sum_{i=0}^{H-1} i \sum_{j=0}^{H-1} R(i, j); \mu_y = \sum_{i=0}^{H-1} j \sum_{j=0}^{H-1} R(i, j) \\ \sigma_x^2 &= \sum_{i=0}^{H-1} (I_x(i) - \mu_x(i))^2; \sigma_y^2 = \sum_{j=0}^{H-1} (I_y(j) - \mu_y(j))^2 \end{aligned}$$

3.2.5 Inverse difference moment

Inverse Difference Moment (IDM) is the local homogeneity which is used to compute the relationship of pixels [28]. Suppose, if local gray level is consistent and inverse GLCM is high, then it is high.

$$IDM = \sum_{i=0}^{H-1} \sum_{j=0}^{H-1} \frac{R(i, j)}{1 + (i-j)^2} \quad (6)$$

IDM weight value is the inverse of the Contrast weight.

3.2.6 Sum of squares, variance

Sum of squares is an arithmetical procedure which is employs in regression investigation for to establish the distribution of data position.

$$Variance = \sum_{i=0}^{H-1} \sum_{j=0}^{H-1} (i - \mu)^2 R(i, j) \quad (7)$$

This attribute situates comparatively high weights on the components that diverge from the standard value of $R(i, j)$

3.2.7 Sum average

$$Average = \sum_{i=0}^{2H-1} i R_{x+y}(i) \quad (8)$$

μ = The GLCM mean (being an estimate of the intensity of all pixels in the relationships that contributed to the GLCM).

Here, the entire 112 attributes are removed for every image block which is exploited for the segmentation by means of proposed FCM related segmentation process.

3.3 FbFCM-WOA based segmentation

Segmentation of medical ultrasound images at low dissimilarity and intensity inhomogeneity environment are considered as a demanding task. Fuzzy clustering is generally exploited for image segmentation problem in medical image assessment. Fuzzy C-means (FCM) clustering is a data clustering procedure. Here, each data position encompasses a cluster position in its association esteem. Additionally, the data components are encompass a position through further than one group which is derived from the level of association for the data position to each cluster [22]. Fuzzy C means is dividing an input vectors as precise fuzzy cluster and get a cluster center in every cluster through the target where an expenditure of discrepancy measure is inadequate. Suppose, if the essential quantity of data component cluster is pre-determined then the fuzzy C-means clustering is expensive. The flowchart of proposed FbFCM-WOA related segmentation process is specified in beneath Fig. 2.

Moreover, the input data is classified as quantity of clusters indiscriminately and the centroid is engendering the clusters for the period of clustering. Here, the clusters are modernized by the association position of data position and the innovative centroid is resolute at iteration. But, the unsystematic initialization of preliminary cluster centroid is direct to local minima and computational ineffectiveness. Besides, the conventional fuzzy clustering policy is considered as a remarkable method for image segmentation problem because it facilitates pixels to be congregated as several clusters [8].

Therefore, we have proposed an effectual FbFCM-WOA related segmentation process for the appropriate segmentation of kidney tumor/cyst. FbFCM-WOA is used to enhance the presentation of conventional FCM through supporting the preliminary centroids by means of Whale optimization algorithm. So, it develops its general computational presentation. Besides, the foremost dissimilarity of proposed attribute related FCM is carrying out segmentation by the attribute's removal at the block stage rather than the pixel intensity.

3.3.1 FbFCM algorithmic steps

Here, consider the $U = \{u_1, u_2, u_3, \dots, u_m\}$ is the input group of attributes in every image block and $W = \{w_1, w_2, w_3, \dots, w_n\}$ is the group of cluster centers, the FbFCM clustering algorithm is carry out by the subsequent steps.

- Step 1: In this step, choose 'n' cluster centroids as randomly. At this point, the quantity of clusters is created as three. Therefore, $n = 3$ and $W = \{w_1, w_2, w_3\}$ is the attribute vector of one 3×3 sub-image block. Here, the termination threshold β , fuzzy exponent x and preliminary association matrix $S^{(0)} = [0]$ are also established.
- Step 2: Calculate the fuzzy association ' λ_{jk} ' as:

$$\lambda_{jk} = \frac{1}{\sum_{l=1}^n \left(\frac{r_{jk}}{r_{jl}} \right)^{\frac{2}{x-1}}} \quad (9)$$

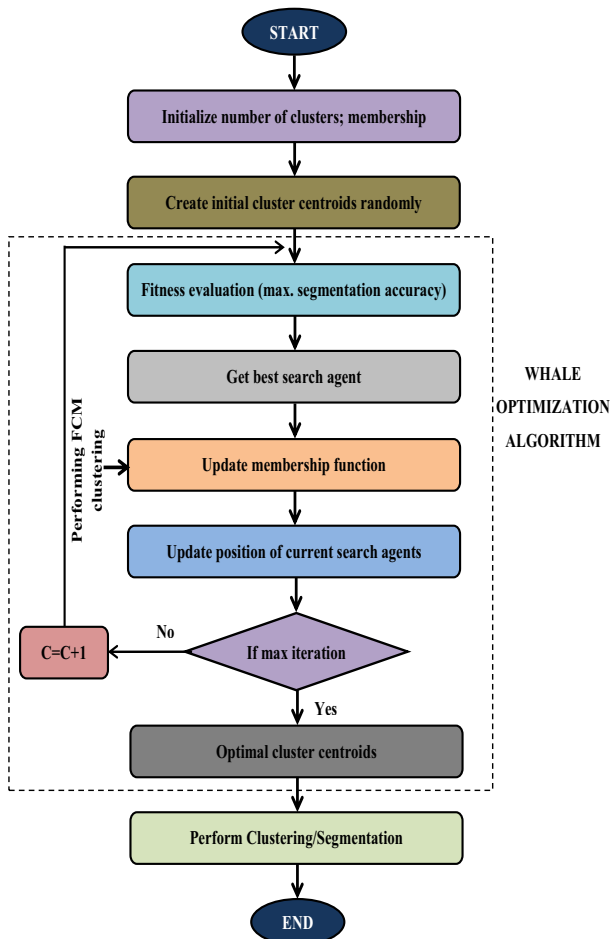


Fig. 2 Flowchart of proposed FbFCM-WOA based segmentation method

Step 3: Schedule the fuzzy centroids ' w_k ' as

$$w_k = \frac{\left(\sum_{j=1}^m (\lambda_{jk})^x u_j \right)}{\left(\sum_{j=1}^m (\lambda_{jk})^x \right)} \quad (10)$$

Step 4: Here, replicate the step 2 and 3 in anticipation of the least intention task ' O ' value is accomplished or $\|S^{(l+1)} - S^{(l)}\| < \beta$

In the above equations,

l	is the current iteration.
β	is the termination criterion between $[0,1]$.
$S = [\lambda_{jk}]_{m \times n}$	is the fuzzy membership matrix.
O	is the objective function, which can be written as [22],

$$\min O_x(S, W) = \sum_{j=1}^m \sum_{k=1}^n \lambda_{jk}^x r^2(u_j, w_k)$$

Where, $r_{jk}^2(u_j, w_k) = \|u_j - w_k\|$ represents the distance between (u_j, w_k) .

Therefore, the clustered outputs are acquired in the execution where the segmented section is notable. The proposed segmentation method is utilizing Whale optimization algorithm for choose the finest centroids and develop the presentation of FCM by the centroid collection [4].

3.3.2 Steps involved in FbFCM-WOA

The proposed FbFCM-WOA method is establishing the optimization step at the FCM related clustering. At this point, the proposed FbFCM-WOA method is indiscriminately initializes a group of cluster centroids in iteration which is derived from the intention task (i.e. the maximum segmentation accuracy) and choose the finest centroid groups. Afterward, the FCM related segmentation is prepared and the association matrix is modernized by the finest centroid group at iteration. The WOA process is briefly depicted in the subsequent segment.

I. Whale optimization algorithm The whale optimization algorithm (WOA) is a recent meta-heuristic algorithm which is offered by means of Mirjalili and Lewis. It employs search mediator for to choose the universal optimum for optimization problem [1]. The WOA is generally stimulates the humpback whales hunting procedure which is also known as bubble-net hunting process. They usually hunt the krill or little fishes close to the surface. In this method, the humpback whales are swim in the region of prey at reduction circle with a spiral-shaped path for to create unique bubbles as circle or '9'-shaped path [12].

Generally, this algorithm integrates three operators such as the search for prey (exploration phase), the encircling prey, and the bubble-net foraging (exploitation phase) which are take place by humpback whales. The arithmetical representation of Whale Optimization algorithm (WOA) is specified in below segment:

Step 1: Initialization

Initialize the whale populace as $S_i (i = 1, 2, 3, \dots, m)$, the limitation u , coefficient U and V , the greatest quantity of iteration $MaxIter$ and the iteration counter x . Establish the populace N (i.e. N set of cluster centroids) is engendered indiscriminately and every search mediator S_i (i.e. one set of cluster centroids) in the populace is estimated by means of fitness task $f(S_i)$

Step 2: Fitness function

The fitness task is used to establish the finest explanation. In proposed optimization difficulty, the fitness task is used to estimate the greatest exactness of segmentation.

$$f(S_i) = \max(\text{segmentation accuracy}) = \frac{TP + TN}{TP + TN + FN + FP} \quad (11)$$

Where, TP-True Positive; TN- True Negative; FN-false Negative and; FP- False Positive.

Step 3: Encircling prey

Humpback whale is surrounding the prey (little fishes) and modernize its location to the finest array with the duration of increasing quantity of iteration from instigate to a maximum quantity of iteration.

$$\vec{A} = \left| V \cdot \vec{S}^*(x) - S(x) \right| \quad (12)$$

$$\vec{S}(x+1) = \vec{S}^*(x) - \vec{U} \cdot \vec{A} \text{ if } d < 0.5 \quad (13)$$

Where,

\vec{U}, \vec{A} are coefficient vectors,
 x is a current iteration,
 $\vec{S}^*(x)$ is position vector of the optimum solution so far and
 $S(x)$ is position vector
 d expresses random number between [0, 1].

Coefficient vectors \vec{U}, \vec{A} are calculated as follows:

$$\vec{U} = 2\vec{u} * r - \vec{u} \quad (14)$$

$$\vec{V} = 2 * r \quad (15)$$

Where,

\vec{u} is a variable linearly decrease from 2 to 0 over the course of iteration.
 r is a random number [0,1].

Step 4: Bubble-net attacking method

Here, the arithmetical equations of bubble-net activities in humpback whales are containing two procedures which are specified as:

- **Shrinking encircling mechanism**

The method is exploiting by means of reducing the value from 2 to 0. An unsystematic value of vector is expanded among $[-1, 1]$.

- **Spiral updating position**

Arithmetical spiral equation of location refresh among humpback whale and prey was helix-shaped expansion which is specified as:

$$\vec{S}(x+1) = \vec{A}' * e^{bx} * \cos(2\pi l) + \vec{S}^*(x) \text{ if } d \geq 0.5 \quad (16)$$

Where,

l is a random number $[-1, 1]$,
 b is constant that defines the shape of logarithmic spiral,
 $\vec{A}' = |\vec{S}^*(x) - S(x)|$ expresses the distance between i^{th} whale to the prey mean the best solution so far. [25]

- **Search for prey**

The vector \vec{A} is exploiting to observe the prey; vector \vec{A} is obtaining the values as more remarkable than one or not precisely - 1.

Exploration takes after two conditions

$$\vec{A} = \left| \vec{V} \cdot \vec{S}_{rand} - \vec{S} \right| \quad (17)$$

$$\vec{S}(x+1) = \vec{S}_{rand} - \vec{U} \cdot \vec{A} \quad (18)$$

At long last takes after these conditions:

$|\vec{U}| > 1$ is exploiting WOA algorithm for to determine the universal finest deliberate detachment from local optima

$|\vec{U}| < 1$ is updating the location of existing seek agent/finest array as preferred [23].

Step 5: **Termination**

In iteration, the output cluster centroids are verified by means of preceding finest cluster centroids. Suppose, if the acquired cluster centroids at recent iteration is enhanced than the preceding finest cluster centroids then the FCM related segmentation is completed. If not, the WOA algorithm is attempts to develop the recent explanation through the subsequent steps 3 and 4.

Finally, the WOA algorithm is stopped when the segmentation accuracy is improved.

Pseudocode of FbFCM-WOA

```

Initialization the whale population,  $S_i (i = 1, 2, 3, \dots, m)$  //initial cluster
centroids

Initialize u, U, and V;  $S^*$  = the best search agent

Calculate the fitness of each search agent

Procedure WOA (Population,  $u, U, V, MaxIter, \dots$ )

    x=1

    While  $x \leq maxIter$  (or)  $\|S^{(l+1)} - S^{(l)}\| < \beta$  do

        for each search agent do

            if  $|U| \leq 1$  then

                Update the position of the current search agent using (13) and
(16)

            else if  $|U| > 1$  then

                Select a random search agent  $S_r$  and

                Update the position of the current search agent using (18)

            end if

        end for

        Update u, U, and V

        Update  $S^*$  if there is a better solution

    Update fuzzy membership function

    x=x+1

    end while

    return  $S^*$ 

end procedure

```

4 Result and discussion

In this segment, the result and discussion regarding the proposed Feature related fuzzy C-means- Whale optimization Algorithm (FB-FCM-WOA) is illustrated which employs for kidney cysts and tumor ultra sound image segmentation. In proposed method, the Whale optimization Algorithm is exploiting for the optimization of cluster centroids in Fuzzy C-means. The proposed method is implemented by means of MATLAB software and the analysis is accomplished through a system which containing 8 GB RAM and 3.60 GHz Intel i-3 processor.

Here, the consequences are examined by means of the obtainable procedure with dissimilar standard evaluation metrics such as like sensitivity, specificity, accuracy; Positive Predictive Value (PPV) and Negative Predictive Value (NPV) which are investigated to illustrate the presentation of segmentation process. Additionally, we contrasted the obtainable process of Feature related K-means clustering (FB-K-means), Feature related Fuzzy C-means clustering (FB-FCM), Intensity related K-means clustering (IB-K-means), and Intensity related Fuzzy C-means clustering (IB-FCM) through proposed process Feature related fuzzy C-means- Whale optimization Algorithm (FB-FCM-WOA).

4.1 Evaluation metrics

Here, the presentation of system is computed by means of standard statistical metrics which encompasses sensitivity, selectivity, Accuracy, Positive Predictive Value (PPV) and Negative Predictive Value (NPV). Some of the standard count values are True Positive (TP), True Negative (TN), False Positive (FP) and False Negative (FN) which are depicted as below.

4.1.1 Sensitivity

Sensitivity is the experiment that will choose ‘disease’ from those with the disease:

$$\text{Sensitivity} = A/(A + C) \times 100$$

4.1.2 Specificity

Specificity is the division of without disease who will contain a negative experiment result:

$$\text{Specificity} = D/(D + B) \times 100$$

4.1.3 Accuracy

Accuracy is also known as “diagnostic accuracy” or “diagnostic effectiveness” which is the proportion of appropriately categorized subjects from the entire subjects:

$$\text{Accuracy} = (A + D)/(A + B + C + D) \times 100$$

4.1.4 Positive Predictive Value (PPV)

The fraction of positive experiment consequences which are considered as the Positive Predictive Value

$$PPV = A / (A + B) \times 100$$

4.1.5 Negative Predictive Value (NPV)

The fraction of negative experiment consequences which are considered as the Negative Predictive Value

$$NPV = D / (D + C) \times 100$$

Here, A is True Positive, B is a False Positive, C is a False Negative and D is a True Negative.

4.2 Performance analysis

The presentation evaluation of proposed FB-FCM-WOA algorithm is investigated and contrasted by the obtainable process of diverse kidney cyst and tumor ultrasound images. The proposed process is illustrated by means of obtainable process (FB-FCM, FB-K-means, IB-FCM and IB-K-means) with dissimilar parametric. We compute the standard value of metrics for to illustrate the proposed process which is best contrast to further process.

The segmented of kidney cyst ultra sound images for C_8 was illustrated below in the Fig. 3.

The segmentation of kidney tumor ultra sound images for T_1 was illustrated below in the Fig. 4.

4.2.1 Performance measures

Here, we estimate the metrics value for every image by means of dissimilar process. The estimated value of True Positive (TP), True Negative (TN), False Positive (FP), False Negative (FN), sensitivity, specificity, accuracy; Positive Predictive Value (PPV) and Negative Predictive Value (NPV) are listed.

The estimated metrics value for every image by means of feature related Fuzzy C-means process (FB-FCM) is specified in the Table 1.

Here, the Table 1 is illustrates about the True Positive (TP), True Negative (TN), False Positive (FP), and False Negative (FN), sensitivity, specificity, accuracy, Positive Predictive Value (PPV) and Negative Predictive Value (NPV) values for Feature related Fuzzy C-means (FB-FCM) process.

From the above Table 1, the computed value of True Positive high is 3904 in the C_12 image, the computed value of True Negative high is 63,444 in the T_1 image, the computed value of False Positive low is 28 in the C_13, the computed value of False Negative low is 0 in the T_4 image, the computed value of sensitivity high is 1 in the T_4 image, the computed value of specificity high is 0.999 in the C_13 image, the computed value of accuracy high is 0.995 in the C_8 image, the computed value of PPV high is 0.979 in the C_13 image, and the computed value of NPV high is 1 in the T_4 image by means of FB-FCM process.

The estimated metrics value for every image by means of Feature related K-means (FB-K-means) process is specified in the Table 2.

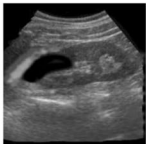
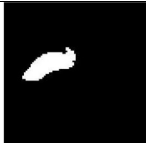
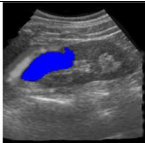

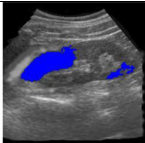


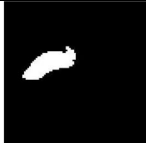
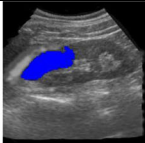
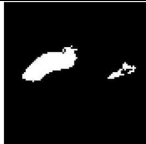
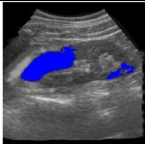
Input C_8 image	Method	Segmented output	Segmented portion marked in original image
	FB-FCM		
	FB-K-means		
	IB-FCM		
	IB-K-means		
	FB-FCM-WOA		

Fig. 3 Segmentation result for C_8 ultra sound image using different techniques

Here, the Table 2 is illustrates about the True Positive (TP), True Negative (TN), False Positive (FP), and False Negative (FN), sensitivity, specificity, accuracy, Positive Predictive Value (PPV) and Negative Predictive Value (NPV) values for Feature Based K-means (FB-K-means) process.

From the above Table 2, the computed value of True Positive high is 4357 in the C_12 image, T the computed value of rue Negative high is 64,922 in the T_2 image, the computed value of False Positive low is 4 in the T_1, the computed value of False Negative low is 1 in the T_4 image, the computed value of sensitivity high is 0.999 in the T_4 image, the computed value of specificity high is 0.999 in the T_1 image, the computed value of accuracy high is

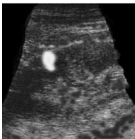

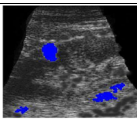
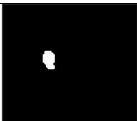


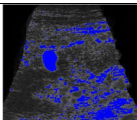

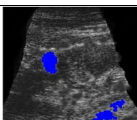


Input T_1 image	Method	Segmented output	Segmented portion marked in original image
	FB-FCM		
	FB-K- means		
	IB-FCM		
	IB-K- means		
	FB-FCM- WOA		

Fig. 4 Segmentation result for T_1 ultra sound image using different techniques

Table 1 The FB-FCM method with different metric value for kidney cyst and tumor image

FB-FCM									
Image	TP	TN	FP	FN	Sensitivity	specificity	accuracy	PPV	NPV
C_10	3468	61,483	330	255	0.931507	0.994661	0.991074	0.913112	0.99587
C_12	3904	60,479	137	1016	0.793496	0.99774	0.982407	0.966098	0.983478
C_13	1331	62,566	28	1611	0.452413	0.999553	0.974991	0.979397	0.974898
C_8	2903	62,342	67	224	0.928366	0.998926	0.99556	0.977441	0.99642
C_9'	2645	59,752	2701	438	0.857931	0.956751	0.952103	0.494762	0.992723
T_1	794	63,444	1293	5	0.993742	0.980027	0.980194	0.38045	0.999921
T_2	557	60,527	4445	7	0.987589	0.931586	0.932068	0.111355	0.999884
T_3	513	59,211	5795	17	0.967925	0.910854	0.911316	0.081325	0.999713
T_4'	1233	58,624	5679	0	1	0.911684	0.913345	0.178385	1
Average					0.879219	0.964643	0.959229	0.564703	0.993657

Table 2 The FB-K-means method with different metric value for kidney cyst and tumor image

FB-K-means									
Image	TP	TN	FP	FN	Sensitivity	specificity	accuracy	PPV	NPV
C_10	3699	59,455	2358	24	0.993554	0.961853	0.963654	0.610698	0.999596
C_12	4357	60,176	440	563	0.885569	0.992741	0.984695	0.908276	0.990731
C_13	0	62,261	333	2942	0	0.99468	0.950027	0	0.954879
C_8	2990	61,781	628	137	0.956188	0.989937	0.988327	0.826423	0.997787
C_9'	2916	58,925	3528	167	0.945832	0.94351	0.943619	0.452514	0.997174
T_1	660	64,733	4	139	0.826033	0.999938	0.997818	0.993976	0.997857
T_2	451	64,922	50	113	0.799645	0.99923	0.997513	0.9002	0.998262
T_3	512	59,813	5193	18	0.966038	0.920115	0.920486	0.089746	0.999699
T_4'	1232	63,324	979	1	0.999189	0.984775	0.985046	0.557214	0.999984
Average					0.819117	0.976309	0.970132	0.593228	0.992886

0.997 in the T_1 image, the computed value of PPV high is 0.993 in the T_1 image, and the computed value of NPV high is 0.999 in the T_4 image by means of FB-K-means process.

The estimated metrics value for every image by means of Intensity related Fuzzy C-means process (IB-FCM) is specified in the Table 3.

Here, the Table 3 illustrates about the True Positive (TP), True Negative (TN), False Positive (FP), and False Negative (FN), sensitivity, specificity, accuracy, Positive Predictive Value (PPV) and Negative Predictive Value (NPV) values for Intensity related Fuzzy C-means (IB-FCM) process.

From the above Table 3, the computed value of True Positive high is 3340 in the C_12 image, the computed value of True Negative high is 55,057 in the T_1 image, the computed value of False Positive low is 7447 in the C_12, the computed value of False Negative low is 0 in the T_4 image, the computed value of sensitivity high is 1 in the T_4 image, the computed value of specificity high is 0.8771 in the C_12 image, the computed value of accuracy high is 0.862 in the C_12 image, the computed value of PPV high is 0.309 in the C_12 image, and the computed value of NPV high is 1 in the T_4 image by means of IB-FCM process.

The estimated metrics value for every image by means of Intensity related K-means (IB-K-means) process is specified in the Table 4.

Here, the Table 4 illustrates about the True Positive (TP), True Negative (TN), False Positive (FP), and False Negative (FN), sensitivity, specificity, accuracy, Positive Predictive

Table 3 The IB-FCM method with different metric value for kidney cyst and tumor image

IB-FCM									
Image	TP	TN	FP	FN	Sensitivity	specificity	accuracy	PPV	NPV
C_10	0	41,637	20,176	3723	0	0.673596	0.63533	0	0.917923
C_12	3340	53,169	7447	1580	0.678862	0.877145	0.862259	0.309632	0.971141
C_13	0	51,821	10,773	2942	0	0.827891	0.790726	0	0.946278
C_8	2460	49,454	12,955	667	0.786697	0.792418	0.792145	0.159585	0.986692
C_9'	2519	47,260	15,193	564	0.817061	0.756729	0.759567	0.14222	0.988207
T_1	799	55,057	9680	0	1	0.850472	0.852295	0.076248	1
T_2	563	50,820	14,152	1	0.998227	0.782183	0.784042	0.03826	0.99998
T_3	530	51,707	13,299	0	1	0.795419	0.797073	0.038325	1
T_4'	1233	51,932	12,371	0	1	0.807614	0.811234	0.090635	1
Average					0.697872	0.795941	0.787186	0.09499	0.978914

Table 4 The IB-K-means method with different metric value for kidney cyst and tumor image

IB-K-means									
Image	TP	TN	FP	FN	Sensitivity	specificity	accuracy	PPV	NPV
C_10	3376	40,883	20,930	347	0.906796	0.661398	0.675339	0.138896	0.991584
C_12	3481	52,890	7726	1439	0.70752	0.872542	0.860153	0.310609	0.973513
C_13	0	51,899	10,695	2942	0	0.829137	0.791916	0	0.946354
C_8	2547	49,013	13,396	580	0.814519	0.785351	0.786743	0.159757	0.988305
C_9'	2775	45,014	17,439	308	0.900097	0.720766	0.729202	0.137281	0.993204
T_1	793	57,976	6761	6	0.992491	0.895562	0.896744	0.104977	0.999897
T_2	558	54,712	10,260	6	0.989362	0.842086	0.843353	0.051581	0.99989
T_3	529	56,831	8175	1	0.998113	0.874242	0.875244	0.060777	0.999982
T_4'	1233	61,288	3015	0	1	0.953113	0.953995	0.290254	1
Average					0.8120998	0.826022	0.823633	0.139348	0.988082

Value (PPV) and Negative Predictive Value (NPV) values for Intensity related K-means (IB-K-means) process.

From the above Table 4, the computed value of True Positive high is 3481 in the C_12 image, the computed value of True Negative high is 61,288 in the T_1 image, the computed value of False Positive low is 3015 in the T_4 image, the computed value of False Negative low is 0 in the T_4 image, the computed value of sensitivity high is 1 in the T_4 image, the computed value of specificity high is 0.953 in the T_4 image, the computed value of accuracy high is 0.953 in the T_4 image, the computed value of PPV high is 0.290 in the T_4 image, and the computed value of NPV high is 1 in the T_4 image by means of IB-K-means process.

The estimated metrics value for every image by means of Feature related Fuzzy C-means-Whale optimization algorithm (FB-FCM-WOA) process is specified in the Table 5.

Here, the Table 5 is illustrating about the True Positive (TP), True Negative (TN), False Positive (FP), and False Negative (FN), sensitivity, specificity, accuracy, Positive Predictive Value (PPV) and Negative Predictive Value (NPV) values for the proposed Feature related Fuzzy C-means – whale optimization Algorithm (FB-FCM-WOA) process.

From the above Table 5, the computed value of True Positive high is 4482 in the C_12 image, the computed value of True Negative high is 64,733 in the T_1 image, the computed value of False Positive low is 4 in the T_1, the computed value of False Negative low is 2 in the T_4 image, the computed value of sensitivity high is 0.998 in the T_1 image, the

Table 5 The proposed FB-FCM-WOA method with different metric value for kidney cyst and tumor image

FB-FCM-WOA									
Image	TP	TN	FP	FN	Sensitivity	specificity	accuracy	PPV	NPV
C_10	3459	61,510	303	264	0.929089	0.995098	0.991348	0.919458	0.995726
C_12	4482	59,266	1350	438	0.910976	0.977729	0.972717	0.768519	0.992664
C_13	2640	62,399	195	302	0.897349	0.996885	0.992416	0.931217	0.995183
C_8	2990	61,781	628	137	0.956188	0.989937	0.988327	0.826423	0.997787
C_9'	2916	58,925	3528	167	0.945832	0.94351	0.943619	0.452514	0.997174
T_1	660	64,733	4	139	0.826033	0.999938	0.997818	0.993976	0.997857
T_2	524	64,642	330	40	0.929078	0.994921	0.994354	0.613583	0.999382
T_3	429	64,370	636	101	0.809434	0.990216	0.987228	0.340933	0.996887
T_4'	1231	63,540	763	2	0.998378	0.988134	0.988327	0.617352	0.999969
Average					0.911373	0.986263	0.984017	0.718219	0.996959

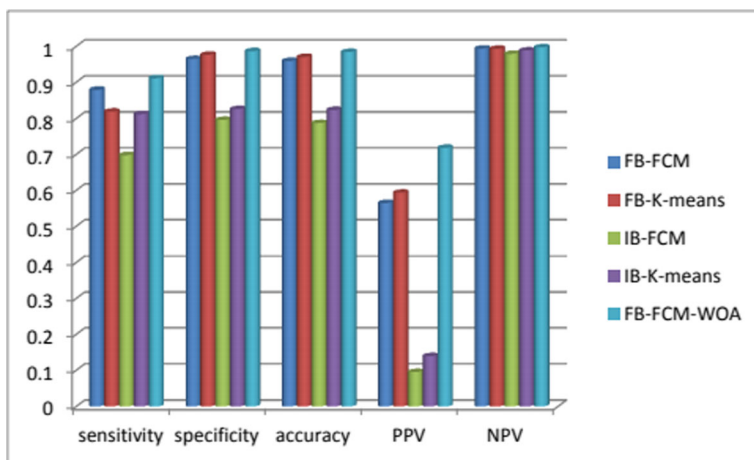


Fig. 5 The proposed method compared with existing method

computed value of specificity high is 0.999 in the T_1 image, the computed value of accuracy high is 0.988 in the T_4 image, the computed value of PPV high is 0.993 in the T_1 image, and the computed value of NPV high is 0.999 in the T_4 image by means of FB-FCM-WOA process.

Here, we also compute the standard value for sensitivity, specificity, accuracy, Positive Predictive Value (PPV) and Negative Predictive Value (NPV). The standard value of the entire metrics is illustrating about the evaluation chart of proposed process through obtainable process. The evaluation chart is specified as beneath Fig. 3.

From the above Fig. 5, the evaluation of proposed process FB-FCM-WOA among obtainable processes of FB-FCM, FB-K-means, IB-FCM and IB-K-means are depicted. The proposed process is augmented when contrast to the obtainable process by means of dissimilar metrics like sensitivity, specificity, accuracy, Positive Predictive Value (PPV) and Negative Predictive Value (NPV). The proposed FB-FCM-WOA (91.1%, 98.6%, and 98.4%) sensitivity, specificity and accuracy are better than obtainable process. The PPV and NPV (71.8% and 99.6%) are also better than the obtainable process.

5 Conclusion

In this document, we have enhanced an effectual segmentation process by the help of GLCM feature extraction which is employs for every sub image of ultrasound kidney image. The proposed FBFCM-WOA is optimally choosing the cluster centroids by the exactness of segmentation consequences. The presentation of proposed segmentation process is contrasted by means of obtainable process like FB-FCM, FB-K-means, IB-FCM, and IB-K-means process. Additionally, it is computed by means of diverse presentation metrics like sensitivity, specificity, accuracy; Positive Predictive Value (PPV) and Negative Predictive Value (NPV). From the consequences, it is observed that the standard exactness of proposed process is 98%, whereas it is less for further process.

Publisher's note Springer Nature remains neutral with regard to jurisdictional claims in published maps and institutional affiliations.

References

- Aljarah I, Faris H, Mirjalili S (2018) Optimizing connection weights in neural networks using the whale optimization algorithm. *Soft Comput* 22(1):1–15
- Attia MW et al. (2015) "Classification of ultrasound kidney images using PCA and neural networks." *IJACSA* International Journal of Advanced Computer Science and Applications 6.4
- Chao J, Shi F, Xiang D, Jiang X, Zhang B, Wang X, Zhu W, Gao E, Chen X (2016) 3D fast automatic segmentation of kidney based on modified AAM and random forest. *IEEE Trans Med Imaging* 35(6):1395–1407
- Ding M, Fan G (2016) Articulated and generalized gaussian kernel correlation for human pose estimation. *IEEE Trans Image Process* 25(2):776–789
- Divya KK, Akkala V, Bharath R, Rajalakshmi P, Mohammed AM, Merchant SN, Desai UB (2016) Computer aided abnormality detection for kidney on FPGA based IoT enabled portable ultrasound imaging system. *Irbm* 37(4):189–197
- Gayathri K, Vasanthi D (2017) Brain Tumor Segmentation Using K-Means Clustering and Fuzzy C-Means Algorithms
- Goceri N, Goceri E (2015) "A neural network based kidney segmentation from MR images." *Machine Learning and Applications (ICMLA)*, 2015 IEEE 14th International Conference on. IEEE
- Guo L et al (2017) Image guided Fuzzy C-means for image segmentation. *Int J Fuzzy Syst* 19(6):1660–1669
- Hong S, Kang W, Zhang Q, Wang S (2015) Kidney segmentation in CT sequences using SKFCM and improved GrowCut algorithm. *BMC Syst Biol* 9(5):S5
- Jin C et al (2017) Fast segmentation of kidney components using random forests and ferns. *Med Phys* 44(12):6353–6363
- Kairuddin WNH, Mahmud WMHW (2017) Texture Feature Analysis for Different Resolution Level of Kidney Ultrasound Images. *IOP Conference Series: Materials Science and Engineering*. Vol. 226. No. 1. IOP Publishing
- Kaveh A, Ilchi Ghazaan M (2017) Enhanced whale optimization algorithm for sizing optimization of skeletal structures. *Mech Based Des Struct Mach* 45(3):345–362
- Khalifa F et al. (2016) A random forest-based framework for 3D kidney segmentation from dynamic contrast-enhanced CT images. *Image Processing (ICIP)*, 2016 IEEE International Conference on. IEEE
- Kirubha V, Manju Priya S (2016) Survey on Data Mining Algorithms in Disease Prediction. *Int J Comput Trends Tech* 38(3):24–128
- Ladumor DP et al. (2016) A whale optimization algorithm approach for unit commitment problem solution. *Proc. National Conf. Advancement in Electrical & Power Electronics Engineering (AEPEE 2016)*, Morbi, India
- Lee, L-K, Liew S-C (2015) "A survey of medical image processing tools." In *Software Engineering and Computer Systems (ICSECS)*, 2015 4th International Conference on, pp. 171–176. IEEE
- Lin D-T, Lei C-C, Hung S-W (2006) Computer-aided kidney segmentation on abdominal CT images. *IEEE Trans Inf Technol Biomed* 10(1):59–65
- Mahdi M, Plataniotis KN, Stergiopoulos S (2017) An automated approach for kidney segmentation in three-dimensional ultrasound images. *IEEE j biomed health inform* 21(4):1079–1094
- Mahmud W, Hafizah WM (2013) Kidney Abnormality Detection and Classification Using Ultrasound Vector Graphic Image Analysis. *Diss. Universiti Teknologi Malaysia*
- Mary JM (2017) Image Segmentation Technique-A study on Region Growing Approaches
- Pawar MP, Mulla AN (2017) Design and Analysis Performance of Kidney Cyst Detection from Ultrasound Images
- Pugazhenthir D (2016) "Breast Abnormalities Detection in Digital Mammogram Using Fuzzy C-Means Clustering and Support Vector Machine-Matlab Implementation." *Breast* 4.2
- Sharawi M, Zawbaa HM, Emary E (2017) "Feature selection approach based on whale optimization algorithm." *Advanced Computational Intelligence (ICACI)*, 2017 Ninth International Conference on. IEEE
- Torres HR et al. (2018) "Kidney Segmentation in Ultrasound, Magnetic Resonance and Computed Tomography Images: A Systematic Review." *Computer Methods and Programs in Biomedicine*
- Trivedi IN et al. (2016) Novel adaptive whale optimization algorithm for global optimization. *Indian Journal of Science and Technology* 9.38
- Velmurugan V, Arunkumar M, Gnanasivam P (2017) A review on systemic approach of the ultra sound image to detect renal calculi using different analysis techniques. *Biosignals, Images and Instrumentation (ICBSII)*, 2017 Third International Conference on. IEEE
- Xie X, Liu S, Yang C, Yang Z, Xu J, Zhai X (2017) The application of smart materials in tactile actuators for tactile information delivery. *arXiv preprint arXiv:1708.07077*



Paladugu Raju was born in 1982 and received his B.Tech degree from Nagarjuna University in the year 2003 and received M.E degree in the year 2008 from Andhra University. He is a Ph.D Scholar of JNTUK Kakinada. He is currently working as an Assistant Professor, Department of ECE in GITAM Institute of Technology, GITAM University Vishakhapatnam. His research area is Image Processing.



Dr. Veera Malleswara Rao received his B.E. degree from Andhra University In the year 1985 and received M.E. degree in the year 1989 from Andhra University and completed his Ph.D from J.N.T.U Hyderabad. He has 23 years of teaching experience, 8 years of Research Experience and currently working in GITAM Institute of Technology, GITAM University, Visakhapatnam as Professor. He completed one UGC project. He produced 6 PhD's and guiding 20 PhD scholars He is a life member of AMIE. Area of interests are related to Low Power VLSI Design, Microwave, Image processing.



Dr. Bhima Prabhakara Rao received his B.Tech degree in Electronics and Communications Engineering, M.Tech degree in Electronics and Communication Systems from SVUniversity, Tirupati in 1979, 1981 respectively and received the Ph.D degree from IISC, Bangalore in 1995. Dr. B. Prabhakara Rao has more than 28 years of experience in teaching and 20 years of R & D. He is an expert in Signal Processing & Communications. He produced 9 PhD's and guiding 35 PhD scholars. He held different positions in his career like Head of the Department, Vice Principal, in JNTU College of Engineering, Director (Institute of Science & Technology) and Director of Evaluation; Director of Foreign University & Alumni Relations and Rector in the Newly Established JNT University Kakinada. He authored 17 Titles of Books. He published more than 120 technical papers in National and International journals and conferences. Interests are in coding theory, information theory, Image Processing, Optical Communications, Microwave Communications, Satellite Communications and Signal processing